Hindawi
Journal of Nanomaterials
Volume 2022, Article ID 6484573, 6 pages
https://doi.org/10.1155/2022/6484573

Research Article

Preparation and Characterization of Magnesium Oxide Nanoparticles and Its Application for Photocatalytic Removal of Rhodamine B and Methylene Blue Dyes

Jayakaran Pachiyappan,[1] Nirmala Gnanansundaram,[2] Selvaraju Sivamani,[1] Naveen Prasad Balakrishna Pillai Sankari,[1] Nachiappan Senthilnathan,[1] and Gizachew Assefa Kerga[3]

[1]*Engineering Department, University of Technology and Applied Sciences, Salalah, Oman*
[2]*School of Chemical Engineering, Vellore Institute of Technology, Vellore, India*
[3]*Department of Chemical Engineering, College of Biological and Chemical Engineering, Addis Ababa Science and Technology University, Addis Ababa, Ethiopia*

Correspondence should be addressed to Nirmala Gnanansundaram; gsnirmala@vit.ac.in
and Gizachew Assefa Kerga; gizachew.assefa@aastu.edu.et

Received 11 May 2022; Accepted 1 July 2022; Published 28 July 2022

Academic Editor: R Lakshmipathy

In this research work, MgO nanoparticles were synthesized by a single-step coprecipitation approach using *Kappaphycus alvarezii* extract as stabilizer. The synthesized MgO nanoparticles exhibit cubic crystal structure, which were confirmed by XRD and FTIR. The purity of MgO nanomaterials was confirmed by P-XRD. The diffraction crests of MgO nanomaterials are in accordance with customary patterns of pure MgO (JCPDS No.00–004-0821). Electron microscopic analysis demonstrated the appearance of MgO nanoflakes. The UV-DRS was used to calculate the optical band gap of MgO nanoparticles and found to be 4.71 eV. MgO nanoparticles have substantial photocatalytic activity for the deterioration of rhodamine B (RhB) and methylene blue (MB) dyes under visible light irradiation. The experimental data fitted first-order kinetics and around >95% degeneration of both dyes was achieved by photocatalysis using synthesized MgO nanoparticles. Thus, the data obtained from this research can effectively be utilized in large-scale industrial applications during wastewater treatments.

1. Introduction

Nanodimensional metals and metal oxides have ushered in a new era of materials in material chemistry due to their large variety of applications [1]. In the field of carcinogenic dye removal in wastewater treatment, synthetic dyes are becoming the subject of research. Therefore, researchers seek a cost-effective and efficient method to decompose such a hazardous dye [2]. Photocatalytic degradation of dyes using UV/sunlight is one of the most preferred methods since the reactions are conducted using renewable solar energy that is both inexpensive and simple [3].

MgO is increasingly utilized in the production of magnesium batteries, biosensors, toxic metal ion sensors, catalysts, superconducting goods, refractory additives, and toxic wastewater treatment [4]. Metal oxides such as ZnO, CuO, MnO_2, TiO_2, and CoO_2 can be found. The multifunctional properties of MgO, such as its nontoxicity, environmental friendliness, high-specific surface area, exceptional biocompatibility, and global availability of its source, have sparked the interest of young researchers worldwide [5]. MgO NPs have been manufactured using high-temperature solid state synthesis, sol–gel method, vapor phase oxidation, and pulsed laser deposition [6, 7].

While these techniques are effective, they are often prohibitively expensive and require lengthy experimental procedures. As a result, a simple, time-saving, and cost-effective synthesis technique is needed [8]. Metal nitrates and suitable reducing agents undergo an exothermic redox reaction in solution, which has been utilized to successfully manufacture nanoscale metal oxides [9].

Photocatalysis is one of the most promising wastewater treatment techniques as it provides almost complete removal of pollutants. Photocatalysts are performed using materials with specific characteristics. Nanomaterials are mostly preferred photocatalysts for removal of pollutants. The partial reduction of graphene oxide (GO) in aqueous extract of the red macroalgae *K. alvarezii* (Phycosap) containing flavonols and transition metals was documented for use as a liquid fertilizer [10]. Literature studies reveal the synthesis of MgO nanoparticles by template free approach [11] and characterized for microstructure and optical properties [12]. Also, the researchers studied the application of photocatalysis of textile and tannery effluents using MgO nanoparticles [13] and the impact of annealing temperature on photocatalysis [14].

MgO nanoparticles synthesized from *Dalbergia sissoo* [15], *Artemisia abrotanum* [16], *Sargassum wightii* [17], and *Saussurea costus* [18]. Photocatalysis using UVA-LED light source also has been studied [19]. Apart from the synthesis of nanoparticles, ZrO_2 nanoparticles and mixed MgO-ZnO nanoparticles were utilized for photocatalysis of dyes [20, 21]. Also, Congo red and other dyes are also effectively removed by photocatalysis [22, 23]. For the analysis of literature, *K. alvarezii* has not been studied for the synthesis of MgO nanoparticles. Hence, the aim of the present research is to synthesize and characterize MgO nanoparticles and its application for photocatalysis of RhB and MB dyes.

2. Materials and Methods

2.1. Materials. All the reagents used in this study are of analar grade (commercially available high purity) from Merck and Sd-fine, India. SRL in Mumbai provided the silica gel. Sigma-Aldrich provided the industrial dyes (RhB and Methylene blue). Throughout the study, Milli-Q (Millipore) water was used. All weights were taken using an analytical balance (Shimadzu, Japan).

2.2. Preparation of MgO Nanoparticles. Magnesium nitrate as precursors, marine red alga as a stabilizing agent, and NaOH as a reducing agent were used in a coprecipitation technique to produce MgO nanoparticles. 1/10 M of $MgNO_3$ was added to 40 mL of aqueous extract of *K. alvarezii* and stirred vigorously for 45 min. Later, 2/10 M NaOH was dropped into the mixture till the development of a turbid precipitate. Additionally, the solution was kept at 25 ± 3°C to remove the precipitates. The precipitated nanoparticles were washed three times with distilled water and then dried and calcined at 873 K for four hours in a muffle furnace.

2.3. Characterization of MgO Nanoparticles. Powder X-ray diffraction patterns (P-XRD) of MgO nanoparticles were acquired with a Bruker, Germany diffractometer operating at 40 kV and 30 mA with a $CuK_{\alpha 1}$ radiation source. The surface morphology of NPs was determined by SEM analysis (FEI QUANTA-200). Dry samples of MgO NPs were placed into the carbon-coated copper grid and picturized. Energy dispersive analysis of X-rays (EDAX) was performed to analyze the elemental composition in the samples.

2.4. Preparation Stock Dye Solution. A stock dye (MB and RhB) solution of 100 ppm was prepared by dissolving 100 mg of dye in 1000 mL of double-distilled water. The standard flask was kept for complete mixing in magnetic stirrer. From the stock solution, 100 mL standard solutions of required concentrations (5-20 ppm) were prepared.

2.5. Batch Photocatalysis Studies. In 100 mL of MB and RhB dye solution with a defined concentration (5–20 ppm), 100–500 mg of MgO NPs were disseminated and subjected to visible light while swirling continuously. Withdrawing a certain volume of the exposed solution (10 mL), every 15 min, was used to measure the absorbance spectra of the samples. By centrifuging the solution, we were able to separate the MgO NPs and evaluate their deterioration. A spectrophotometer at 664 and 554 nm was used (MB and RhB, respectively) to evaluate the degradation rate of the dye. Equation (1) was used to calculate the percentage of dye degradation.

$$\%\text{degradation} = \left(\frac{C_i - C_e}{C_i}\right) \times 100, \quad (1)$$

where C_i and C_e (mg/L) are the initial and equilibrium metal concentrations, respectively, and V is volume of solution taken.

3. Results and Discussion

3.1. Characterization of MgO Nanoparticles. P-XRD was used to evaluate the purity and crystallinity of MgO NPs (Figure 1(a)). The diffraction peaks of MgO NPs are compared to normal patterns of JCPDS No. 00–004-0821, which are in close alignment with the recorded 2θ values. $CuK\alpha_1$ radiation ($\lambda = 1.5406$ Å), 40 kV-40 mA, and 2θ scanning mode are used to examine the X-ray diffraction patterns of NPs. The data was taken in the range of 20 to 100 degrees. *Miller indices* are group of three numbers that indicates the orientation of a plane or set of parallel planes of atoms in a crystal. Miller indices ($h = 2$, $k = 2$, and $l = 0$) are used to identify the peaks, and the resulting P-XRD spectrum shows that the synthesized NPs are crystalline in nature. The active composition of MgO is shown by the large peaks of P-XRD. The crystallinity was calculated using the FWHM (full width at half maximum) values. With fewer impurities, the real volume fraction of the nanocomposites agrees with the patterns obtained from P-XRD. The purity and crystallinity of MgO were found to be good [10].

Due to the major alcoholic O-H functional group, which is the key absorption point of shifted metal ions, FTIR analysis revealed a broad range between 3492 cm^{-1} and 2945 cm^{-1} [24]. The vibration modes of –CN and CO= produced peaks at 1752 cm^{-1} and 1487 cm^{-1}, respectively (Figure 1(b)). The

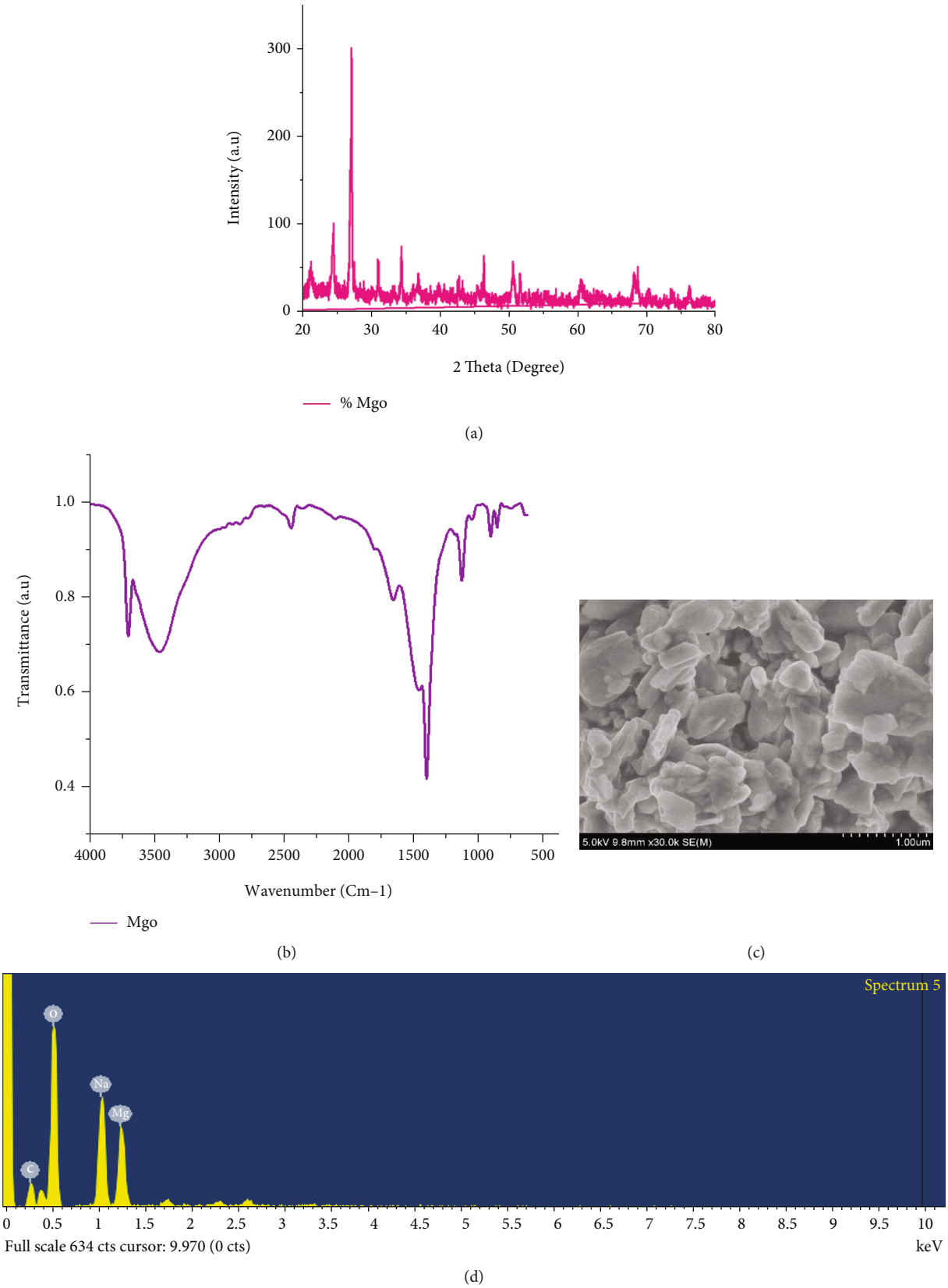

Figure 1: (a) P-XRD, (b) FTIR, (c) SEM, and (d) EDAX of MgO nanoparticles.

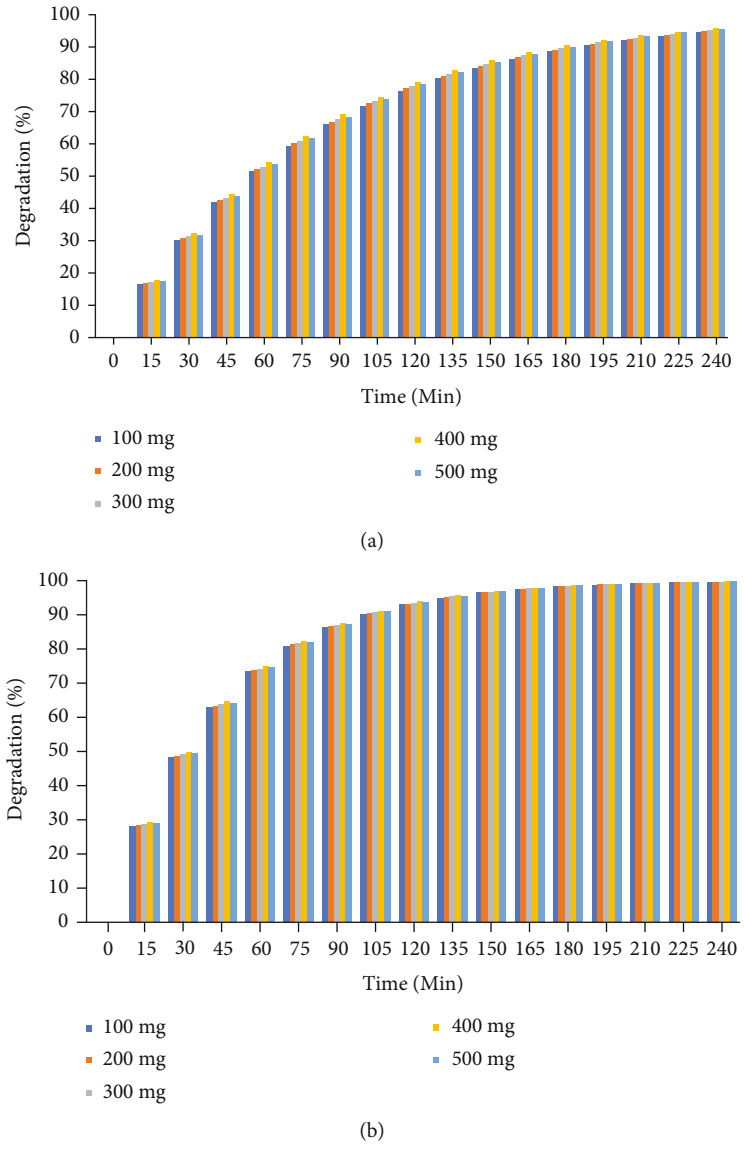

Figure 2: Photocatalytic degradation of (a) rhodamine B and (b) methylene blue dyes.

peak at 1287 cm^{-1} may be explained by the bending vibration of the OH bond, which is associated with the water surface absorbed by the produced MgO nanoparticles. The peaks at 843 cm^{-1} and 562 cm^{-1} may be related to Mg-O bonding, which contribute to the formation of pure and synthetic metal oxides.

The HR-SEM micrograph of MgO nanoparticles (Figure 1(c)) reveals flake-like morphology with diameters ranging from 52 to 68 nm, and the corresponding EDAX graph (Figure 1(d)) revealed the existence of elements such as Mg and O, confirming the development of pure MgO nanoparticles. MgO NP showed plain surface mechanism due to porous behaviour, and thereby, composite existence is observed in HR-SEM. Porous habitat of the MgO NPs evidence the relative adsorption onto its acquainted surface and henceforth sounds good for the photodegradation of RhB/MB dyes.

3.2. Batch Photocatalysis Studies. The photocatalytic degradation of RhB and MB dyes over pristine MgO NPs as photocatalysts are shown in Figures 2(a) and 2(b), respectively. It exhibited significant RhB/MB photocatalysis till 240 min of light enlightenment, which proved that the RhB/MB is stable. After 150 min of illumination, the pristine MgO photocatalyst degraded >95% for RhB and >99% for MB solution. Further, the pristine MgO NPs exhibited an excellent photodegradation of MB dye over RhB. The photodegradation of RhB over MgO NPs was found to be 94% after 180 min. The photodegradation of MB over MgO NPs was found to be 98%, respectively, after 150 min. The MB dye exhibited a higher photodegradation than the RhB dye. Photodegradation increases with an increase in time which may be due to an enhancement of the absorption of photons.

The effect of nanocomposite dosage on the photodegradation of RhB/MBn dyes was analyzed. The photocatalyst dosage of 400 mg was found to produce maximum photocatalytic degradation and selected for further experimental studies. The different catalyst concentrations from 100 to 500 mg/L of dye solution indicated that the MgO NPs have shown the increased photodegradation rate with increasing concentration from 100

to 500 mg/L for both the dyes. This enhancement is due to the high surface area of MPs by the huge amounts of dye molecules that can be adsorbed on the surface of the nanocomposite, which makes the nanocomposite potential for the dye degradation efficiency.

Photocurrent response of the MgO NPs with few on/off cycles of the light illumination is performed for RhB and MB dye degradation. The photocurrent response for the MgO NPs exhibited potent enhancement. Hence, the biogenic prepared NPs shows an enhanced charge separation efficiency which may be due to their lower recombination rate of photogenerated charge carriers. From electrochemical impedance spectroscopy EIS measurement, the arc radius of MgO NPs was lesser, indicating a reduced interfacial charge transfer resistance and improved separation effectiveness of photogenerated charge carriers. The numerous parameters such as surface morphology, band gap energy, crystallinity, size of the particle, and defect concentration influenced the photocatalytic performance [25].

The calculated VB and CB edge potentials of the MgO are 1.718 and 3.718 eV, respectively. In the present study, the band energy gap (E_g) values of MgO were slightly different, which may be due to the positive synergistic effect between Mg and O in the NP sample. So, this parameter can be unobserved, but the other parameters were considered. The optimized MgO NP dosage exhibited an enhanced photocatalytic degradation performance of RhB/MB. The degradation of RhB/MB dye molecules on the nanocomposite was facilitated by surface adsorption followed by photocatalysis. Under the visible light irradiation, the electron-hole pair recombination will get reduced leading to an enlarged in the interfacial charge transfer reactions for the degradation of adsorbed RhB/MB molecules. The possible reaction mechanism (2)–(6) of degradation of dye was as follows:

$$\mathrm{MgO} + \mathrm{hv} \longrightarrow \mathrm{e_{CB}}^{-} + \mathrm{h_{VB}}^{+} \quad (2)$$

$$\mathrm{e_{CB}}^{-} + \mathrm{O_2} \longrightarrow \mathrm{O_2}^{-} \quad (3)$$

$$2\mathrm{e_{CB}}^{-} + \mathrm{O_2}^{-} + 2\mathrm{H}^{+} \longrightarrow \mathrm{OH} + \mathrm{OH}^{-} \quad (4)$$

$$\mathrm{h_{VB}}^{+} + \mathrm{H_2O} \longrightarrow \mathrm{H}^{+} + {}^{\bullet}\mathrm{OH} \quad (5)$$

$$\mathrm{RhB/MB} + {}^{\bullet}\mathrm{OH} \longrightarrow \text{Degradation products } (\mathrm{CO_2}, \mathrm{H_2O}, \text{etc.}) \quad (6)$$

In the present investigation, biogenic MgO nanocomposites exhibited an improved photocatalytic degradation of RhB and MB dyes under visible light illumination. Hence, MgO NP was found to be an optimal and efficient photocatalyst for degradation performance, which might be due to the positive synergistic effect and also by reduced recombination of charge carriers. The electrochemical investigation studies were also confirmed the high charge-carrier separation.

4. Conclusion

In this research work, MgO nanoparticles were synthesized by a single-step coprecipitation approach using *K. alvarezii* extract as stabilizer. The synthesized MgO nanoparticles exhibit cubic crystal structure, which were confirmed by XRD and FTIR. The purity of MgO nanomaterials were confirmed by P-XRD. All the diffraction peaks of MgO nanomaterials are in accordance with standard patterns of pure MgO (JCPDS No.00–004-0821). Electron microscopic analysis demonstrated the appearance of MgO nanoflakes. The UV-DRS was used to calculate the optical band gap of MgO nanoparticles and found to be 4.71 eV. MgO nanoparticles have appreciable photocatalytic activity for the degradation of RhB and MB dyes under visible light irradiation. The experimental data fitted first order kinetics and around >95% degeneration of both dyes were achieved by photocatalysis using synthesized MgO nanoparticles. Thus, the data obtained from this research can effectively be utilized in large-scale industrial applications during wastewater treatments.

Data Availability

The underlying data supporting the results of this study are included in this paper.

Conflicts of Interest

The authors declare that they have no conflicts of interest.

References

[1] J. Chen, J. Feng, and W. Yan, "Influence of metal oxides on the adsorption characteristics of PPy/metal oxides for methylene blue," *Journal of Colloid and Interface Science*, vol. 475, article S0021979716302314, pp. 26–35, 2016.

[2] S. K. Alpat, Ö. Özbayrak, Ş. Alpat, and H. Akçay, "The adsorption kinetics and removal of cationic dye, toluidine blue O, from aqueous solution with Turkish zeolite," *Journal of Hazardous Materials*, vol. 151, no. 1, article S0304389407008205, pp. 213–220, 2008.

[3] E. Altıntıg, H. Altundag, M. Tuzen, and A. Sarı, "Effective removal of methylene blue from aqueous solutions using magnetic loaded activated carbon as novel adsorbent," *Chemical Engineering Research and Design*, vol. 122, article S0263876217301788, pp. 151–163, 2017.

[4] M. K. Dahri, L. B. L. Lim, M. R. R. Kooh, and C. M. Chan, "Adsorption of brilliant green from aqueous solution by unmodified and chemically modified Tarap (Artocarpus odoratissimus) peel," *International journal of Environmental Science and Technology*, vol. 14, no. 12, article 1347, pp. 2683–2694, 2017.

[5] H. L. Ding, Y. X. Zhang, S. Wang, J. M. Xu, S. C. Xu, and G. H. Li, "Fe3O4@ SiO2 core/shell nanoparticles: the silica coating regulations with a single core for different core sizes and shell thicknesses," *Chemistry of Materials*, vol. 24, no. 23, pp. 4572–4580, 2012.

[6] C. J. Rhodes, "Eating small: applications and implications for nanotechnology in agriculture and the food industry," *Science Progress*, vol. 97, no. 2, pp. 173–182, 2014.

[7] V. K. Garg and N. Kataria, "Nanomaterial-based sorbents for the removal of heavy metal ions from water," *Advanced Nanomaterials for Wastewater Remediation*, vol. 179, 2016.

[8] S. K. Sharma, *Heavy Metals in Water: Presence, Removal and Safety*, Royal Society of Chemistry, United Kingdom, 2014.

[9] M. Sharma, D. Mondal, A. K. Das, and K. Prasad, "Production of partially reduced graphene oxide nanosheets using a seaweed sap," *RSC Advances*, vol. 4, no. 110, pp. 64583–64588, 2014.

[10] H. M. Cai, G. J. Chen, C. Y. Peng et al., "Removal of fluoride from drinking water using tea waste loaded with Al/Fe oxides: a novel, safe and efficient biosorbent," *Applied Surface Science*, vol. 328, article S0169433214026634, pp. 34–44, 2015.

[11] K. Mageshwari, S. S. Mali, R. Sathyamoorthy, and P. S. Patil, "Template-free synthesis of MgO nanoparticles for effective photocatalytic applications," *Powder Technology*, vol. 249, article S0032591013005937, pp. 456–462, 2013.

[12] G. Balakrishnan, R. Velavan, K. M. Batoo, and E. H. Raslan, "Microstructure, optical and photocatalytic properties of MgO nanoparticles," *Results in Physics*, vol. 16, article 103013, Article ID S221137971933493X, 2020.

[13] A. Fouda, S. E. D. Hassan, E. Saied, and M. F. Hamza, "Photocatalytic degradation of real textile and tannery effluent using biosynthesized magnesium oxide nanoparticles (MgO-NPs), heavy metal adsorption, phytotoxicity, and antimicrobial activity," *Journal of Environmental Chemical Engineering*, vol. 9, no. 4, article S2213343721003237, p. 105346, 2021.

[14] P. Diana, S. Saravanakumar, K. H. Prasad et al., "Enhanced photocatalytic decomposition efficacy of novel MgO NPs: impact of annealing temperatures," *Journal of Inorganic and Organometallic Polymers and Materials*, vol. 31, no. 7, article 1896, pp. 3027–3036, 2021.

[15] M. I. Khan, M. N. Akhtar, N. Ashraf et al., "Green synthesis of magnesium oxide nanoparticles using Dalbergia sissoo extract for photocatalytic activity and antibacterial efficacy," *Applied Nanoscience*, vol. 10, no. 7, article 1414, pp. 2351–2364, 2020.

[16] R. Dobrucka, "Synthesis of MgO nanoparticles using Artemisia abrotanum herba extract and their antioxidant and photocatalytic properties," *Iranian Journal of Science and Technology, Transactions A: Science*, vol. 42, no. 2, article 76, pp. 547–555, 2018.

[17] A. Pugazhendhi, R. Prabhu, K. Muruganantham, R. Shanmuganathan, and S. Natarajan, "Anticancer, antimicrobial and photocatalytic activities of green synthesized magnesium oxide nanoparticles (MgONPs) using aqueous extract of Sargassum wightii," *Journal of Photochemistry and Photobiology B: Biology*, vol. 190, article S1011134418312090, pp. 86–97, 2019.

[18] M. Amina, N. M. Al Musayeib, N. A. Alarfaj et al., "Biogenic green synthesis of MgO nanoparticles using Saussurea costus biomasses for a comprehensive detection of their antimicrobial, cytotoxicity against MCF-7 breast cancer cells and photocatalysis potentials," *PLoS One*, vol. 15, no. 8, article e0237567, 2020.

[19] S. Akbari, G. Moussavi, and S. Giannakis, "Efficient photocatalytic degradation of ciprofloxacin under UVA-LED, using S, N-doped MgO nanoparticles: synthesis, parametrization and mechanistic interpretation," *Journal of Molecular Liquids*, vol. 324, article S0167732220370732, p. 114831, 2021.

[20] G. Rajesh, S. Akilandeswari, D. Govindarajan, and K. Thirumalai, "Enhancement of photocatalytic activity of ZrO_2 nanoparticles by doping with Mg for UV light photocatalytic degradation of methyl violet and methyl blue dyes," *Journal of Materials Science: Materials in Electronics*, vol. 31, no. 5, pp. 4058–4072, 2020.

[21] S. Vishwanathan and S. Das, "Glucose-mediated one-pot hydrothermal synthesis of hollow magnesium oxide-zinc oxide (MgO-ZnO) microspheres with enhanced natural sunlight photocatalytic activity," in *Environmental Science and Pollution Research*, pp. 1–14, Springer, 2022.

[22] M. I. Din, R. Khalid, J. Najeeb, and Z. Hussain, "Fundamentals and photocatalysis of methylene blue dye using various nanocatalytic assemblies-a critical review," *Journal of Cleaner Production*, vol. 298, article S0959652621007873, p. 126567, 2021.

[23] R. Benisha, M. Amalanathan, M. Aravind et al., "Catharanthus roseus leaf extract mediated Ag-MgO nanocatalyst for photocatalytic degradation of Congo red dye and their antibacterial activity," *Journal of Molecular Structure*, vol. 1262, article S0022286022006676, p. 133005, 2022.

[24] C. Xiong, W. Wang, F. Tan, F. Luo, J. Chen, and X. Qiao, "Investigation on the efficiency and mechanism of Cd (II) and Pb (II) removal from aqueous solutions using MgO nanoparticles," *Journal of Hazardous Materials*, vol. 299, article S0304389415006275, pp. 664–674, 2015.

[25] W. Z. Tang and H. An, "UV/TiO_2 photocatalytic oxidation of commercial dyes in aqueous solutions," *Chemosphere*, vol. 31, no. 9, article 004565359580015D, pp. 4157–4170, 1995.